A Cascading Chemical Reporter for *In Situ* Analysis of Cell Envelope Glycan Recycling in Mycobacteria

Amol Arunrao Pohane,[a,†] Devin J. Moore,[b,†] Rebecca A. Gordon,[d] Temitope O. Nathan,[b] Dana M. Gepford,[b] Herbert W. Kavunja,[b] Benjamin M. Swarts,*[,b,c] and M. Sloan Siegrist*[,a,d]

[a]Department of Microbiology, University of Massachusetts, Amherst, MA, USA

[b]Department of Chemistry and Biochemistry, Central Michigan University, Mount Pleasant, MI, USA

[c]Biochemistry, Cell, and Molecular Biology Program, Central Michigan University, Mount Pleasant, MI, 48859 United States

[d]Molecular and Cellular Biology Graduate Program, University of Massachusetts, Amherst, MA, USA

[†]These authors contributed equally to this work.

*Corresponding authors: siegrist@umass.edu; ben.swarts@cmich.edu

Abstract

In mycobacteria, the glucose-based disaccharide trehalose cycles between the cytoplasm, where it is a stress protectant and carbon source, and the cell envelope, where it is released as a by-product of outer mycomembrane glycan biosynthesis and turnover. Trehalose recycling via the LpqY-SugABC transporter promotes virulence, antibiotic recalcitrance, and efficient adaptation to nutrient deprivation. The source(s) of trehalose and the regulation of recycling under these and other stressors are unclear. A key technical gap in addressing these questions has been the inability to trace trehalose recycling *in situ*, directly from its site of liberation from the cell envelope. Here we describe a “cascading” chemical reporter that simultaneously marks mycomembrane biosynthesis and subsequent trehalose recycling with alkyne and azide groups. Using this probe, we discovered that the recycling efficiency for trehalose increases upon carbon starvation, concomitant with an increase in LpqY-SugABC expression. The ability of the cascading reporter to probe multiple, linked steps provides a more holistic understanding of mycobacterial cell envelope metabolism and its plasticity under stress.

Main Text and Figures

Mycobacterium is a genus that includes several notorious human and animal pathogens, among them *M. tuberculosis*. These organisms have a distinctive cell envelope featuring a thick and hydrophobic outer membrane, called the mycomembrane, which not only protects against antibiotics and environmental stresses, but also harbors various immunoactive glycolipids[1-8]. Biosynthesis of the mycomembrane (Fig. 1A) is mediated by the non-mammalian disaccharide trehalose, which in the form of trehalose monomycolate (TMM) carries long-chain mycolic acids (MAs) from the cytoplasm to the periplasm. In the periplasm, TMM donates MAs to sugar acceptors, generating the major mycomembrane components trehalose dimycolate (TDM) and arabinogalactan-linked mycolate (AGM)[9]. These reactions, which are catalyzed by antigen 85 (Ag85) mycoloyltransferases, also produce free trehalose, which is recycled by the transporter LpqY-SugABC and then used to regenerate TMM[10,11]. Trehalose is also liberated indirectly, by TDM hydrolase (Tdmh[7,11-13]). Recycled trehalose can be used in central carbon metabolism, as a stress protectant, or directly, in cell surface glycoconjugates such as TMM[14-17]. The recycling of extracytoplasmic trehalose contributes to survival of mycobacteria in macrophages, mice and antibiotics[10,11,18] and promotes resilience to stress under nutrient-limited conditions[11,17]. Since trehalose is released as a by-product of outer mycomembrane glycan biosynthesis or turnover, and enhanced turnover occurs under different stress conditions[7,13,15,19], the source of extracytoplasmic trehalose has been assumed to be turnover[15]. We recently demonstrated that mycomembrane remodeling in carbon-limited *M. smegmatis* and *M. tuberculosis* comprises synthesis in addition to turnover[11], a surprising result given the resource and energy requirements of catabolism. Whether mycomembrane biosynthesis can serve as a source of trehalose for recycling is an open question.

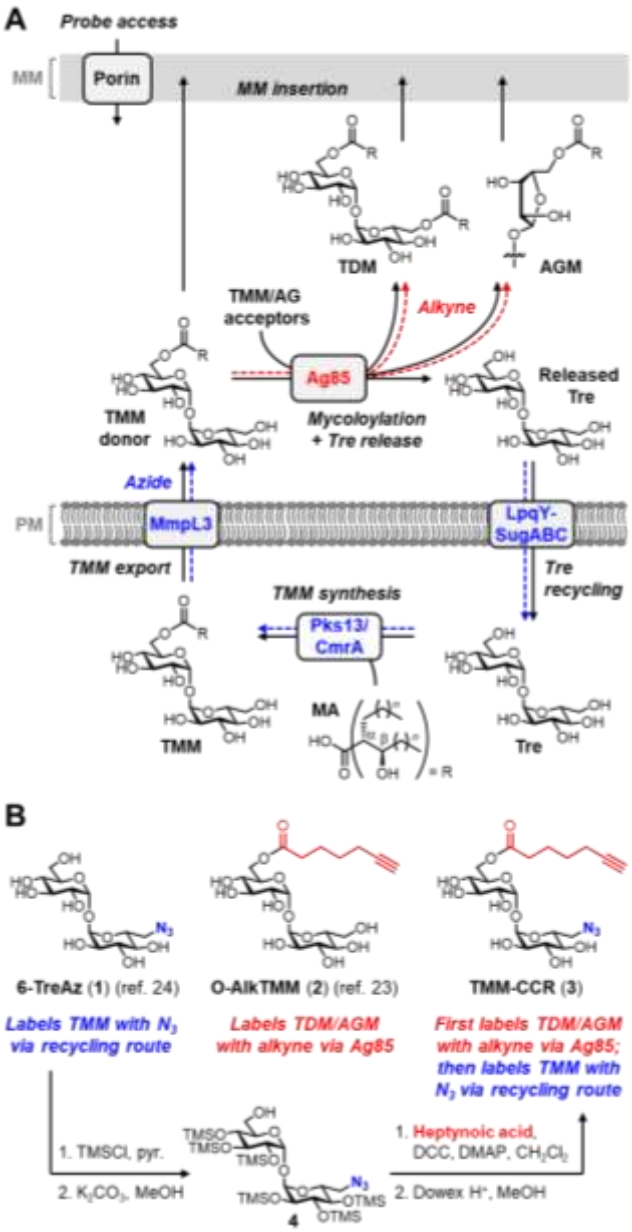

Figure 1. (A) Mycomembrane metabolism. Routes of probe incorporation are shown in blue and red. (B) Chemical reporters used in this study and synthesis of the new cascading reporter TMM-CCR (**3**). Colors correlate reporter group to proposed incorporation route in (A).

Chemical strategies for modifying the bacterial cell surface have a range of applications, including detecting and profiling bacterial cell envelope components, modulating the immunogenicity of the bacterium, and delivering diagnostic or therapeutic chemical cargo specifically to the bacterium[20-23]. Many of these strategies involve metabolic labeling of an envelope component (e.g., glycan, lipid, or protein) with a bioorthogonal functional group,

followed by chemoselective reaction to functionally modify the cell-surface component. Chemical reporters based on biosynthetic precursors for peptidoglycan, lipopolysaccharide, teichoic acids, bacterial glycoproteins, and other components have been valuable tools for studying the cell envelopes of Gram-negative and Gram-positive bacteria[24,25].

We and others have exploited trehalose-mediated mycomembrane construction to create trehalose-based reporters for modifying the cell surface of mycobacteria (Fig. 1B)[25-28]. Following the publication of a fluorescent trehalose analogue that labels mycobacteria via Ag85[28], azide-modified trehalose (TreAz) analogues such as 6-TreAz (**1**) were reported to incorporate into the mycomembrane by LpqY-SugABC-mediated uptake and subsequent elaboration to azide-modified trehalose glycolipids, which can then be functionalized via click chemistry[27]. More recently, we developed TMM-based reporters, including O-AlkTMM (Fig. 1B, (**2**)) and related structures, which deliver bioorthogonal groups to MA acceptors—predominantly the abundant glycolipid AGM, and to a lesser extent trehalose glycolipids and (in some organisms) *O*-mycoloylated proteins[26,29-31]. These and other reporters[12,32,33] are specific for isolated steps of the mycomembrane assembly cycle, *e.g.* Ag85 activity, Tdmh activity, and recycling/TMM synthesis activity. As with other metabolic labeling methods, mycomembrane probes are delivered exogenously, to the outside of cells, likely far in excess of what the bacterium would normally produce and/or incorporate on its own.

Here, we sought to develop a mycomembrane probe that could report multiple, linked steps of mycobacterial mycomembrane metabolism. We designed a bifunctional chemical reporter 6-azido-6-deoxy-6'-*O*-(6'-heptynoyl)-α,α-D-trehalose (Fig. 1B, TMM-CCR (**3**)) that exploits multiple steps in mycomembrane construction to deliver orthogonal alkyne and azide functionalities to the cell surface. We hypothesized that the TMM-mimicking "cascading" chemical reporter TMM-CCR (**3**) would first undergo Ag85-mediated transfer of its heptynoyl chain to MA acceptors, in the process releasing 6-TreAz (**1**), which would then undergo inside-

out incorporation into new TMM via the LpqY-SugABC recycling pathway (Fig. 1A). We anticipated that *in situ* delivery of biosynthetically-derived trehalose, in turn, would enable us to monitor stress-induced recycling in a more precise, physiologically-relevant manner.

The target molecule TMM-CCR (**3**) was chemically synthesized from 6-TreAz (Fig. 1B). To expose the 6-OH group of 6-TreAz for later acylation, it was subjected to per-*O*-trimethylsilylation followed by regioselective 6-*O*-monodesilylation using potassium carbonate in methanol (50% over two steps). Next, alcohol **4** was acylated with heptynoic acid in the presence of DCC and DMAP (81%). Global desilylation with H^+ resin yielded **3** (99%), whose structure and purity were established by NMR and MS. ^{1}H NMR showed downfield-shifted absorptions for the 6'-position hydrogen nuclei, confirming that esterification occurred at the desired site (Supporting Information).

We carried out initial metabolic labeling experiments in *M. smegmatis*, a fast-growing, non-pathogenic organism that is commonly used to model aspects of the mycobacterial cell envelope. First, we tested whether TMM-CCR (**3**) could efficiently deliver both alkynes and azides to the cell surface. *M. smegmatis* was cultured in 50 μM 6-TreAz (**1**), O-AlkTMM (**2**), TMM-CCR (**3**), or left untreated. Cells were washed, fixed, and subjected to standard copper-catalyzed alkyne-azide cycloaddition (CuAAC) to detect incorporated alkynes or azides. Flow cytometry analysis of the labeled cells showed that 6-TreAz and O-AlkTMM were only detected upon CuAAC with carboxyrhodamine 100 alkyne or azide, respectively (Fig. 2A). By contrast, bifunctional reporter TMM-CCR was labeled with fluorophore appended to either functional group, confirming its ability to dual-label the cell surface. Labeling by TMM-CCR was ~35-40% of either 6-TreAz or O-AlkTMM alone (Fig. 2A). These data imply that (*i*) the azide moiety on TMM-CCR decreases TMM-CCR uptake relative to O-AlkTMM and/or O-AlkTMM incorporation by Ag85 but (*ii*) once 6-TreAz is released by Ag85 from TMM-CCR, it is efficiently internalized and incorporated onto the cell surface.

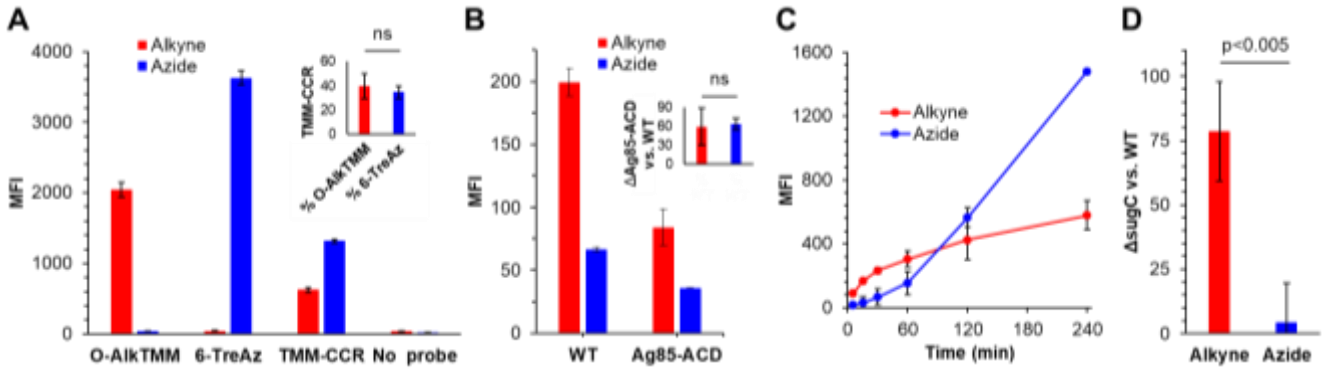

Figure 2. Two-step incorporation of cascading reporter TMM-CCR into the *M. smegmatis* mycomembrane. (A) Labeling of wild-type (WT) *M. smegmatis* with 50 μM O-AlkTMM, 6-TreAz, or TMM-CCR for 15 min or ~10% generation time**.** Alkynes and azides were respectively revealed by CuAAC reaction with complementary azido- or alkynyl-carboxyrhodamine 110 fluorophores. Fluorescence was quantitated by flow cytometry. MFI, median fluorescence intensity. Representative data from five independent experiments performed in triplicate are shown. Inset, TMM-CCR labeling as a % of O-AlkTMM or 6-TreAz over the five experiments. (B) Loss of Ag85ACD decreases both alkyne and azide signal from TMM-CCR. WT and Δ*ag85ACD M. smegmatis* were labeled with TMM-CCR as in (A). Representative data from four independent experiments performed in triplicate are shown. Inset, Δ*ag85ACD* labeling as a % of wild-type (WT) over the four experiments. (C) Time-dependence of alkyne- and azide-derived labeling from TMM-CCR. Wild-type *M. smegmatis* was labeled with TMM-CCR as in Fig. 2A and aliquots were taken at the indicated time points for CuAAC. Data from three independent experiments plotted. (D) Azide but not alkyne signal from TMM-CCR is dependent on the presence of SugC. WT and Δ*sugC M. smegmatis* were labeled as in Fig. 2A. Data (from three independent experiments performed in triplicate) for the mutant were normalized to WT and expressed as fold-change. Statistical significance assessed by two-tailed Student's t test. ns, not significant ($p>0.05$). Error bars, standard deviation of technical or biological replicates as described above.

To test this presumption in more detail, we investigated the pathways by which TMM-CCR incorporated into the cell surface. Pre-incubation of *M. smegmatis* with ebselen, a cysteine-reactive inhibitor of Ag85 activity[26,34], decreased alkyne-derived signal from TMM-CCR as expected (Fig. S1, Supporting Information). However, the azide-derived signal remained unaffected. Although we do not yet understand why 6-TreAz signal does not decline in the presence of ebselen, we hypothesized that there may be compensatory changes in the presence of cysteine-reactive ebselen that could enhance 6-TreAz recovery. Therefore, we compared TMM-CCR labeling in wild-type and ΔAg85-ACD (Δ*MSMEG_6396-6399*) *M. smegmatis*, which lacks three out of five Ag85 enzymes[32]. Both azide- and alkyne-dependent labeling decreased in the mutant strain (Fig. 2B). We next monitored TMM-CCR labeling kinetics in wild-type *M. smegmatis* and found that azide-derived signal lagged alkyne-derived signal at early time points

(Fig. 2C). These experiments, coupled with extensive literature data characterizing similar TMM-based reporters,[29,35-39] support the idea that transfer of the alkyne-terminated acyl chain of TMM-CCR to acceptor molecules, such as arabinogalactan, is catalyzed by Ag85, which in turn liberates 6-TreAz for subsequent incorporation into the mycobacterial cell surface.

Exogenously-added 6-TreAz is recycled by the LpqY-SugABC transporter prior to *M. smegmatis* cell surface incorporation[27]. Therefore, we predicted that labeling by the 6-TreAz released upon the alkyne-terminated acyl chain transfer of TMM-CCR would similarly depend on LpqY-SugABC. We compared TMM-CCR labeling in wild-type and Δ*sugC M. smegmatis*, which lacks a functional trehalose transporter[27]. Only the azide-dependent labeling decreased in the mutant strain (Fig. 2D). These data further support the hypothesis that TMM-CCR undergoes Ag85-mediated alkyne incorporation on the cell surface, thus unmasking 6-TreAz, which then traverses the LpqY-SugABC → Pks13/CmrA → MmpL3 pathway to incorporate into surface TMM from the inside-out[27].

After confirming that bifunctional reporter TMM-CCR efficiently delivers alkynes and azides to the mycomembrane through the expected biosynthetic pathways, we next sought to demonstrate its utility in simultaneous visualization of mycomembrane biosynthesis, marked by its alkyne moiety, and biosynthesis-dependent trehalose recycling, marked by its azide moiety. Mycobacteria are rod-shaped cells that grow from their poles[40,41]. We and others have shown that cell envelope metabolism, including that of the mycomembrane[26,42], occurs primarily at these sites[43-50]. To determine whether TMM-CCR labeling marks active mycomembrane metabolism in *M. tuberculosis*, we first tested whether labeling by the individual O-AlkTMM and 6-TreAz probes was like that of *M. smegmatis*[26,27,42]. As in *M. smegmatis*, labeling with the single probes primarily occurred at the poles of *M. tuberculosis* (Fig. 3A). Alkyne- and azide-dependent labeling with TMM-CCR also occurred at the poles (Figs. 3A, 3B). Unexpectedly, however, labeling was not spatially coincident. These data suggest that the subcellular sites of Ag85-

dependent mycomembrane biosynthesis and trehalose release (O-AlkTMM labeling) are distinct from the sites of trehalose recycling-dependent TMM biosynthesis (6-TreAz labeling) and highlight the ability of TMM-CCR to illuminate multiple, linked steps in mycomembrane metabolism in single *M. tuberculosis* cells.

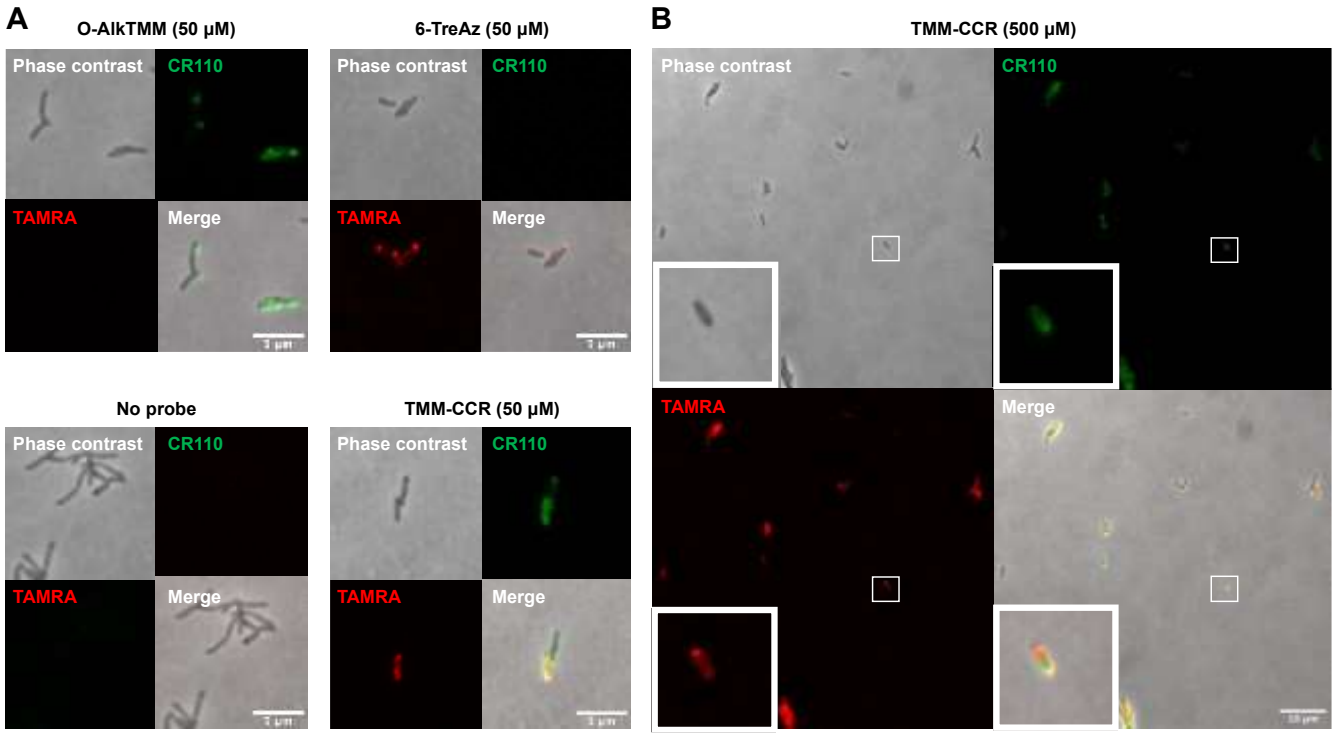

Figure 3. Log-phase Δ*leuD* Δ*panCD M. tuberculosis* (see Supporting Information) was labeled or not overnight with (A) 50 μM of O-AlkTMM, 6-TreAz, or TMM-CCR, or with (B) 500 μM TMM-CCR. After washing, bacteria were fixed in 4% formaldehyde at -20 °C overnight then subjected to successive rounds of CuAAC, the first with 5-TAMRA alkyne, and the second with carboxyrhodamine 110 azide, with washes in between.

We recently demonstrated that non-replicating, carbon-starved *M. smegmatis* and *M. tuberculosis* continue to synthesize AGM[11]. We hypothesized that this final, Ag85-mediated step of mycomembrane catabolism serves as a source of trehalose under these conditions, likely in addition to TDM turnover that we and others have shown occurs in response to various stressors[7,11,13,15,17,19]. To test this hypothesis, we cultured *M. smegmatis* in high or low carbon media and briefly labeled with TMM-CCR. The proportion of azide-dependent signal (6-TreAz-marked trehalose recycling) compared to alkyne-dependent signal (O-AlkTMM-marked AGM biosynthesis) was elevated under carbon-limited conditions (Figs. 4A). This experiment

suggested that a greater proportion of the trehalose liberated from Ag85 activity was recycled upon adaptation to carbon limitation. We next investigated the kinetics of adaptation by transferring *M. smegmatis* from high glucose medium to medium lacking glucose and monitoring azide- and alkyne-derived fluorescence over time. We used *M. smegmatis* pre-adapted to low glucose as a control. Compared to that of pre-adapted *M. smegmatis*, the azide:alkyne ratio of *M. smegmatis* that had been cultured in high glucose prior to transfer increased in the first hour after transfer and plateaued thereafter (Fig. 4B). These data suggest that the efficiency of trehalose capture from AGM biosynthesis increases as *M. smegmatis* adapts to carbon-limited conditions.

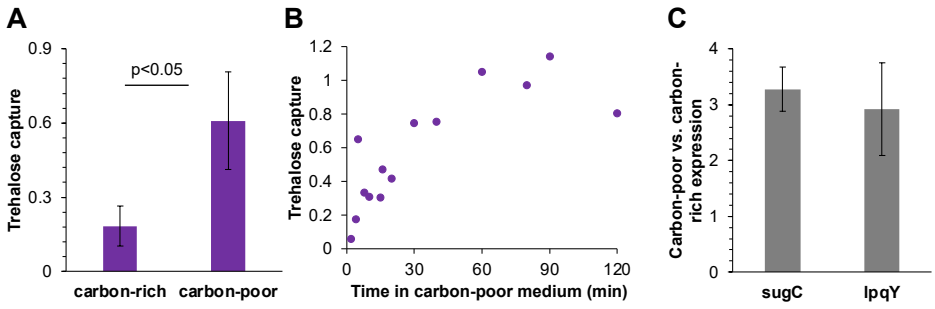

Figure 4. Increased efficiency of trehalose capture from mycomembrane synthesis under glucose limitation. (A) *M. smegmatis* cultured in 0.02% (carbon-poor) or 2% (carbon-rich) glucose as in[11] was labeled with TMM-CCR as in Fig. 2A except that the bacteria were transferred briefly to no-glucose medium to avoid artifactual suppression of O-AlkTMM incorporation into AGM[11]. Data for the azide-derived fluorescence were normalized to alkyne-derived fluorescence ("trehalose capture") and expressed as fold-change from four independent experiments performed in duplicate or triplicate. (B) Rapid increase in trehalose recycling upon adaptation to carbon limitation. *M. smegmatis* cultured in low or high glucose as in Fig. 3A was washed, transferred to no-glucose medium, and labeled with TMM-CCR at indicated time points. Data for the azide-derived fluorescence were normalized to alkyne-derived fluorescence ("trehalose capture"), and data for trehalose capture from carbon-rich *M. smegmatis* were further normalized to *M. smegmatis* that had been pre-adapted, i.e., cultured in carbon-poor medium prior to transfer. Data combined from five independent experiments. Each time point is from 1, 2, or 3 of the independent experiments. (C) The expression of trehalose transporter genes *sugC* and *lpqY* is higher in carbon-poor conditions. Expression monitored by qRT-PCR for *M. smegmatis* cultured in low or high glucose as in Fig. 3A. Data for carbon-limited *M. smegmatis* normalized to *M. smegmatis* cultured in high glucose. Error bars, standard deviation of independent experiments.

Increased recycling could reflect changes in the efficiency or abundance of the LpqY-SugABC transporter. While we have not ruled out the former, the timing of adaptation suggested a role for enhanced transcription/translation of the transporter genes[18,51]. Accordingly, we monitored the mRNA levels of trehalose transporter genes *sugC* and *lpqY* by qRT-PCR.

Consistent with our hypothesis, we found that the relative expression of trehalose transporter increases under carbon limitation (Fig. 4C). As expression of bacterial carbohydrate transporters can be induced by their substrates[52,53], enhanced expression of LpqY-SugABC is also consistent with mycomembrane turnover, which we previously showed occurs in response to carbon limitation and liberates trehalose[11]. Taken together, these data support a model in which mycobacteria make mycomembrane biosynthesis more efficient under carbon limitation by increasing the expression of LpqY-SugABC and extracting a greater proportion of the trehalose by-product.

M. tuberculosis is a pathogen that survives for decades in the hostile, carbohydrate-poor environment of its human host. Illuminating the mechanisms by which mycobacteria survive under stressful conditions has the potential to identify new targets for treatment. Trehalose recycling is known to support mycobacterial survival under stress[10,11,18], but the source of extracellular trehalose in what are presumably slow or non-growing organisms has not been directly characterized, *e.g.* Ag85-mediated biosynthesis or Tdmh-dependent turnover of the mycomembrane. While metabolic labeling can report on trehalose recycling[27], external, in-excess delivery of such probes may or may not recapitulate native flux through the pathway. As well, such strategies do not provide information on the provenance of the free trehalose. Here we addressed this technical gap by synthesizing TMM-CCR, a cascading probe that reports trehalose recycling directly from one of its potential sources, as a by-product of mycomembrane biosynthesis. To our knowledge, this is the first example of a probe that marks multiple metabolic processes with distinct functional groups, i.e., alkyne for cell envelope biosynthesis and azide for cell envelope recycling. Using TMM-CCR, we showed that recycling of biosynthesis-derived trehalose increases under carbon starvation and is likely enabled by increased expression of the transporter. The biosynthetic origin of the recycled trehalose is surprising as *de novo* expansion of the bacterial surface is usually equated with cell replication. While we do not yet know why

carbon-limited *M. smegmatis* and *M. tuberculosis* continue to synthesize mycomembrane, we previously showed that synthesis is part of an overall program of remodeling that also includes turnover and correlates with decreased permeability[11]. Enhanced capture of remodeling by-products enables mycobacteria to “waste not” under unfavorable conditions.

Supporting Information

Supplementary figures, experimental details, and NMR spectra for synthetic compounds.

Acknowledgements

This work was supported by NIH DP2 AI138238 (M.S.S.), NSF CAREER Award 1654408 (B.M.S.), and Camille and Henry Dreyfus Foundation Henry Dreyfus Teacher–Scholar Award TH-17-034 (B.M.S.).

References

(1) Ishikawa, E.; Mori, D.; Yamasaki, S. Recognition of Mycobacterial Lipids by Immune Receptors. *Trends Immunol* 2017, *38* (1), 66.
(2) Daffe, M.; Marrakchi, H. Unraveling the Structure of the Mycobacterial Envelope. *Microbiol Spectr* 2019, *7* (4).
(3) Liu, J.; Rosenberg, E. Y.; Nikaido, H. Fluidity of the lipid domain of cell wall from Mycobacterium chelonae. *Proc Natl Acad Sci U S A* 1995, *92* (24), 11254.
(4) Viswanathan, G.; Joshi, S. V.; Sridhar, A.; Dutta, S.; Raghunand, T. R. Identifying novel mycobacterial stress associated genes using a random mutagenesis screen in Mycobacterium smegmatis. *Gene* 2015, *574* (1), 20.
(5) Sambandan, D.; Dao, D. N.; Weinrick, B. C.; Vilcheze, C.; Gurcha, S. S.; Ojha, A.; Kremer, L.; Besra, G. S.; Hatfull, G. F.; Jacobs, W. R., Jr. Keto-mycolic acid-dependent pellicle formation confers tolerance to drug-sensitive Mycobacterium tuberculosis. *mBio* 2013, *4* (3), e00222.
(6) Lee, W. B.; Kang, J. S.; Choi, W. Y.; Zhang, Q.; Kim, C. H.; Choi, U. Y.; Kim-Ha, J.; Kim, Y. J. Mincle-mediated translational regulation is required for strong nitric oxide production and inflammation resolution. *Nat Commun* 2016, *7*, 11322.
(7) Yang, Y.; Kulka, K.; Montelaro, R. C.; Reinhart, T. A.; Sissons, J.; Aderem, A.; Ojha, A. K. A hydrolase of trehalose dimycolate induces nutrient influx and stress sensitivity to balance intracellular growth of Mycobacterium tuberculosis. *Cell Host Microbe* 2014, *15* (2), 153.

(8) Gebhardt, H.; Meniche, X.; Tropis, M.; Kramer, R.; Daffe, M.; Morbach, S. The key role of the mycolic acid content in the functionality of the cell wall permeability barrier in Corynebacterineae. *Microbiology* 2007, *153* (Pt 5), 1424.
(9) Dulberger, C. L.; Rubin, E. J.; Boutte, C. C. The mycobacterial cell envelope - a moving target. *Nat Rev Microbiol* 2020, *18* (1), 47.
(10) Kalscheuer, R.; Weinrick, B.; Veeraraghavan, U.; Besra, G. S.; Jacobs, W. R., Jr. Trehalose-recycling ABC transporter LpqY-SugA-SugB-SugC is essential for virulence of Mycobacterium tuberculosis. *Proc Natl Acad Sci U S A* 2010, *107* (50), 21761.
(11) Pohane, A. A.; Carr, C. R.; Garhyan, J.; Swarts, B. M.; Siegrist, M. S. Trehalose Recycling Promotes Energy-Efficient Biosynthesis of the Mycobacterial Cell Envelope. *mBio* 2021, *12* (1).
(12) Holmes, N. J.; Kavunja, H. W.; Yang, Y.; Vannest, B. D.; Ramsey, C. N.; Gepford, D. M.; Banahene, N.; Poston, A. W.; Piligian, B. F.; Ronning, D. R.et al. A FRET-Based Fluorogenic Trehalose Dimycolate Analogue for Probing Mycomembrane-Remodeling Enzymes of Mycobacteria. *ACS Omega* 2019, *4* (2), 4348.
(13) Ojha, A. K.; Trivelli, X.; Guerardel, Y.; Kremer, L.; Hatfull, G. F. Enzymatic hydrolysis of trehalose dimycolate releases free mycolic acids during mycobacterial growth in biofilms. *J Biol Chem* 2010, *285* (23), 17380.
(14) Nobre, A.; Alarico, S.; Maranha, A.; Mendes, V.; Empadinhas, N. The molecular biology of mycobacterial trehalose in the quest for advanced tuberculosis therapies. *Microbiology* 2014, *160* (Pt 8), 1547.
(15) Eoh, H.; Wang, Z.; Layre, E.; Rath, P.; Morris, R.; Branch Moody, D.; Rhee, K. Y. Metabolic anticipation in Mycobacterium tuberculosis. *Nat Microbiol* 2017, *2*, 17084.
(16) Shleeva, M. O.; Trutneva, K. A.; Demina, G. R.; Zinin, A. I.; Sorokoumova, G. M.; Laptinskaya, P. K.; Shumkova, E. S.; Kaprelyants, A. S. Free Trehalose Accumulation in Dormant Mycobacterium smegmatis Cells and Its Breakdown in Early Resuscitation Phase. *Front Microbiol* 2017, *8*, 524.
(17) Lee, J. J.; Lee, S. K.; Song, N.; Nathan, T. O.; Swarts, B. M.; Eum, S. Y.; Ehrt, S.; Cho, S. N.; Eoh, H. Transient drug-tolerance and permanent drug-resistance rely on the trehalose-catalytic shift in Mycobacterium tuberculosis. *Nat Commun* 2019, *10* (1), 2928.
(18) Danelishvili, L.; Shulzhenko, N.; Chinison, J. J. J.; Babrak, L.; Hu, J.; Morgun, A.; Burrows, G.; Bermudez, L. E. Mycobacterium tuberculosis Proteome Response to Antituberculosis Compounds Reveals Metabolic "Escape" Pathways That Prolong Bacterial Survival. *Antimicrob Agents Chemother* 2017, *61* (7).
(19) Galagan, J. E.; Minch, K.; Peterson, M.; Lyubetskaya, A.; Azizi, E.; Sweet, L.; Gomes, A.; Rustad, T.; Dolganov, G.; Glotova, I.et al. The Mycobacterium tuberculosis regulatory network and hypoxia. *Nature* 2013, *499* (7457), 178.
(20) Siegrist, M. S.; Swarts, B. M.; Fox, D. M.; Lim, S. A.; Bertozzi, C. R. Illumination of growth, division and secretion by metabolic labeling of the bacterial cell surface. *FEMS Microbiol Rev* 2015, *39* (2), 184.
(21) Behren, S.; Westerlind, U. Glycopeptides and -Mimetics to Detect, Monitor and Inhibit Bacterial and Viral Infections: Recent Advances and Perspectives. *Molecules* 2019, *24* (6).
(22) Dutta, A. K.; Choudhary, E.; Wang, X.; Zahorszka, M.; Forbak, M.; Lohner, P.; Jessen, H. J.; Agarwal, N.; Kordulakova, J.; Jessen-Trefzer, C. Trehalose Conjugation Enhances Toxicity of Photosensitizers against Mycobacteria. *ACS Cent Sci* 2019, *5* (4), 644.

(23) Jayawardana, K. W.; Jayawardena, H. S.; Wijesundera, S. A.; De Zoysa, T.; Sundhoro, M.; Yan, M. Selective targeting of Mycobacterium smegmatis with trehalose-functionalized nanoparticles. *Chem Commun (Camb)* 2015, *51* (60), 12028.
(24) Zhang, Z. J.; Wang, Y. C.; Yang, X.; Hang, H. C. Chemical Reporters for Exploring Microbiology and Microbiota Mechanisms. *Chembiochem* 2020, *21* (1-2), 19.
(25) Banahene, N.; Kavunja, H. W.; Swarts, B. M. Chemical Reporters for Bacterial Glycans: Development and Applications. *Chem. Rev.* 2022, *122* (3), 3336.
(26) Foley, H. N.; Stewart, J. A.; Kavunja, H. W.; Rundell, S. R.; Swarts, B. M. Bioorthogonal Chemical Reporters for Selective In Situ Probing of Mycomembrane Components in Mycobacteria. *Angew Chem Int Ed Engl* 2016, *55* (6), 2053.
(27) Swarts, B. M.; Holsclaw, C. M.; Jewett, J. C.; Alber, M.; Fox, D. M.; Siegrist, M. S.; Leary, J. A.; Kalscheuer, R.; Bertozzi, C. R. Probing the mycobacterial trehalome with bioorthogonal chemistry. *J Am Chem Soc* 2012, *134* (39), 16123.
(28) Backus, K. M.; Boshoff, H. I.; Barry, C. S.; Boutureira, O.; Patel, M. K.; D'Hooge, F.; Lee, S. S.; Via, L. E.; Tahlan, K.; Barry, C. E., 3rdet al. Uptake of unnatural trehalose analogs as a reporter for Mycobacterium tuberculosis. *Nat Chem Biol* 2011, *7* (4), 228.
(29) Fiolek, T. J.; Banahene, N.; Kavunja, H. W.; Holmes, N. J.; Rylski, A. K.; Pohane, A. A.; Siegrist, M. S.; Swarts, B. M. Engineering the Mycomembrane of Live Mycobacteria with an Expanded Set of Trehalose Monomycolate Analogues. *ChemBioChem* 2019, *20* (10), 1282.
(30) Kavunja, H. W.; Piligian, B. F.; Fiolek, T. J.; Foley, H. N.; Nathan, T. O.; Swarts, B. M. A chemical reporter strategy for detecting and identifying O-mycoloylated proteins in Corynebacterium. *Chem Commun (Camb)* 2016, *52* (95), 13795.
(31) Kavunja, H. W.; Biegas, K. J.; Banahene, N.; Stewart, J. A.; Piligian, B. F.; Groenevelt, J. M.; Sein, C. E.; Morita, Y. S.; Niederweis, M.; Siegrist, M. S.et al. Photoactivatable Glycolipid Probes for Identifying Mycolate-Protein Interactions in Live Mycobacteria. *J Am Chem Soc* 2020, *142* (17), 7725.
(32) Kamariza, M.; Shieh, P.; Ealand, C. S.; Peters, J. S.; Chu, B.; Rodriguez-Rivera, F. P.; Babu Sait, M. R.; Treuren, W. V.; Martinson, N.; Kalscheuer, R.et al. Rapid detection of Mycobacterium tuberculosis in sputum with a solvatochromic trehalose probe. *Sci Transl Med* 2018, *10* (430).
(33) Hodges, H. L.; Brown, R. A.; Crooks, J. A.; Weibel, D. B.; Kiessling, L. L. Imaging mycobacterial growth and division with a fluorogenic probe. *Proc Natl Acad Sci U S A* 2018, *115* (20), 5271.
(34) Favrot, L.; Grzegorzewicz, A. E.; Lajiness, D. H.; Marvin, R. K.; Boucau, J.; Isailovic, D.; Jackson, M.; Ronning, D. R. Mechanism of inhibition of Mycobacterium tuberculosis antigen 85 by ebselen. *Nat Commun* 2013, *4*, 2748.
(35) Foley, H. N.; Stewart, J. A.; Kavunja, H. W.; Rundell, S. R.; Swarts, B. M. Bioorthogonal chemical reporters for selective in situ probing of mycomembrane components in mycobacteria. *Angew. Chem. Int. Edit.* 2016, *55* (6), 2053.
(36) Kavunja, H. W.; Piligian, B. F.; Fiolek, T. J.; Foley, H. N.; Nathan, T. O.; Swarts, B. M. A chemical reporter strategy for detecting and identifying O-mycoloylated proteins in Corynebacterium. *Chem. Commun.* 2016, *52* (95), 13795.
(37) Kavunja, H. W.; Biegas, K. J.; Banahene, N.; Stewart, J. A.; Piligian, B. F.; Groenevelt, J. M.; Sein, C. E.; Morita, Y. S.; Niederweis, M.; Siegrist, M. S.et al. Photoactivatable Glycolipid Probes for Identifying Mycolate–Protein Interactions in Live Mycobacteria. *J. Am. Chem. Soc.* 2020, *142* (17), 7725.

(38) Hodges, H. L.; Brown, R. A.; Crooks, J. A.; Weibel, D. B.; Kiessling, L. L. Imaging mycobacterial growth and division with a fluorogenic probe. *Proc. Natl. Acad. Sci. U. S. A.* 2018, *115* (20), 5271.
(39) Zhou, X.; Rodriguez-Rivera, F. P.; Lim, H. C.; Bell, J. C.; Bernhardt, T. G.; Bertozzi, C. R.; Theriot, J. A. Sequential assembly of the septal cell envelope prior to V snapping in Corynebacterium glutamicum. *Nat. Chem. Biol.* 2019, *15* (3), 221.
(40) Aldridge, B. B.; Fernandez-Suarez, M.; Heller, D.; Ambravaneswaran, V.; Irimia, D.; Toner, M.; Fortune, S. M. Asymmetry and aging of mycobacterial cells lead to variable growth and antibiotic susceptibility. *Science* 2012, *335* (6064), 100.
(41) Santi, I.; Dhar, N.; Bousbaine, D.; Wakamoto, Y.; McKinney, J. D. Single-cell dynamics of the chromosome replication and cell division cycles in mycobacteria. *Nat Commun* 2013, *4*, 2470.
(42) García-Heredia, A.; Pohane, A. A.; Melzer, E. S.; Carr, C. R.; Fiolek, T. J.; Rundell, S. R.; Lim, H. C.; Wagner, J. C.; Morita, Y. S.; Swarts, B. M.et al. Peptidoglycan precursor synthesis along the sidewall of pole-growing mycobacteria. *Elife* 2018, *7*.
(43) Meniche, X.; Otten, R.; Siegrist, M. S.; Baer, C. E.; Murphy, K. C.; Bertozzi, C. R.; Sassetti, C. M. Subpolar addition of new cell wall is directed by DivIVA in mycobacteria. *Proc Natl Acad Sci U S A* 2014, *111* (31), E3243.
(44) Boutte, C. C.; Baer, C. E.; Papavinasasundaram, K.; Liu, W.; Chase, M. R.; Meniche, X.; Fortune, S. M.; Sassetti, C. M.; Ioerger, T. R.; Rubin, E. J. A cytoplasmic peptidoglycan amidase homologue controls mycobacterial cell wall synthesis. *eLife* 2016, *5*, e14590.
(45) Siegrist, M. S.; Whiteside, S.; Jewett, J. C.; Aditham, A.; Cava, F.; Bertozzi, C. R. (D)-Amino acid chemical reporters reveal peptidoglycan dynamics of an intracellular pathogen. *ACS Chem Biol* 2013, *8* (3), 500.
(46) Botella, H.; Yang, G.; Ouerfelli, O.; Ehrt, S.; Nathan, C. F.; Vaubourgeix, J. Distinct Spatiotemporal Dynamics of Peptidoglycan Synthesis between. *mBio* 2017, *8* (5).
(47) Baranowski, C.; Welsh, M. A.; Sham, L. T.; Eskandarian, H. A.; Lim, H. C.; Kieser, K. J.; Wagner, J. C.; McKinney, J. D.; Fantner, G. E.; Ioerger, T. R.et al. Maturing Mycobacterium smegmatis peptidoglycan requires non-canonical crosslinks to maintain shape. *Elife* 2018, *7*.
(48) Thanky, N. R.; Young, D. B.; Robertson, B. D. Unusual features of the cell cycle in mycobacteria: polar-restricted growth and the snapping-model of cell division. *Tuberculosis (Edinb)* 2007, *87* (3), 231.
(49) Singh, B.; Nitharwal, R. G.; Ramesh, M.; Pettersson, B. M.; Kirsebom, L. A.; Dasgupta, S. Asymmetric growth and division in Mycobacterium spp.: compensatory mechanisms for non-medial septa. *Mol Microbiol* 2013, *88* (1), 64.
(50) Joyce, G.; Williams, K. J.; Robb, M.; Noens, E.; Tizzano, B.; Shahrezaei, V.; Robertson, B. D. Cell division site placement and asymmetric growth in mycobacteria. *PLoS One* 2012, *7* (9), e44582.
(51) Betts, J. C.; Lukey, P. T.; Robb, L. C.; McAdam, R. A.; Duncan, K. Evaluation of a nutrient starvation model of Mycobacterium tuberculosis persistence by gene and protein expression profiling. *Mol Microbiol* 2002, *43* (3), 717.
(52) Titgemeyer, F.; Amon, J.; Parche, S.; Mahfoud, M.; Bail, J.; Schlicht, M.; Rehm, N.; Hillmann, D.; Stephan, J.; Walter, B.et al. A genomic view of sugar transport in Mycobacterium smegmatis and Mycobacterium tuberculosis. *J Bacteriol* 2007, *189* (16), 5903.
(53) Li, M.; Müller, C.; Fröhlich, K.; Gorka, O.; Zhang, L.; Groß, O.; Schilling, O.; Einsle, O.; Jessen-Trefzer, C. Detection and Characterization of a Mycobacterial L-

Arabinofuranose ABC Transporter Identified with a Rapid Lipoproteomics Protocol. *Cell Chem Biol* 2019, *26* (6), 852.